Bulletin of the Seismological Society of America, Vol. 94, No. 3, pp. 856–866, June 2004

Earthquake Relocation Using Cross-Correlation Time Delay Estimates Verified with the Bispectrum Method

by Wen-Xuan Du, Clifford H. Thurber, and Donna Eberhart-Phillips*

Abstract Cross-correlation (CC) determined relative time delays, or related differential travel times, between pairs of seismic events at the same station are often used as input data to improve earthquake relocation results. Researchers generally select those time delays with associated CC coefficients larger than a chosen threshold. When two similar time series are contaminated by correlated noise sources, the relative time delay between them calculated with the CC technique is sometimes not reliable. Noise sources at a station for different events can be partially correlated or just randomly correlated. In this work, we use the bispectrum (BS) method, which works in the third-order spectral domain, to check the reliability of the CC determined time delay. We calculate two time delays with the BS method, one using the band-pass-filtered waveforms and the other with the raw data, and use them to verify (select or reject) the CC estimate computed with the filtered waveforms. We apply this technique to obtain bispectrum-verified CC differential times for 822 New Zealand earthquakes in the Wellington area. Our work demonstrates that the CC time delays verified with the BS method provide improved (smaller root mean square residual and more clustered) earthquake relocation results compared to those selected with the standard threshold criterion.

Introduction

Differential travel times for pairs of seismic events observed at the same station are often calculated by waveform cross-correlation (CC) techniques. These differential times can be used to improve dramatically the earthquake relocation results (Got *et al.*, 1994; Gillard *et al.*, 1996; Shearer, 1997; Rubin *et al.*, 1999; Rowe *et al.*, 2002; Schaff *et al.*, 2002). Researchers often choose those time delay estimates when their associated CC coefficients reach above a specified threshold. For example, Shearer (1997) used the time delays for event pairs with average CC coefficients above 0.45 and with at least 10 estimates having CC coefficients above 0.60. Schaff *et al.* (2002) only chose those estimates with CC values larger than 0.70 and mean coherences above 0.70. The selection of an optimum threshold value is important but difficult. If it is set too high, then only a limited number of very accurate differential times are available to constrain the relative positions of earthquakes. On the other hand, if the threshold value is set too low, then many unreliable time estimates are used and will negatively affect the final relocation result. This is especially so for study regions where the number of stations is relatively small and coverage is not very dense.

When two similar time series are contaminated by correlated noise sources, the time delay estimate between them calculated with the CC technique may not be reliable. Noise at a station for different events can be expected to be partially correlated due to a combination of constant noise sources with time-varying amplitudes (microseisms, wind or cultural noise) and site response effects. They also can be randomly correlated. By working in the third-order spectral domain, the bispectrum (BS) method can eliminate correlated Gaussian noise sources in two similar time series and can be used to obtain the relative time delay between them. It can also suppress non-Gaussian noise with zero skewness (Nikias and Raghuveer, 1987; Nikias and Pan, 1988).

In this work, we use both the CC and BS methods to compute the relative time delay between two windowed waveforms of an event pair recorded at the same station. We do not claim that the BS method always performs better than CC technique; rather, our strategy is to test for agreement between the two methods. CC is performed only on the band-pass-filtered data, while the BS method is applied to both the raw (unfiltered) and filtered waveforms. Because the characteristics of the noise terms in the raw and filtered data are different, the two BS time delay estimates may not always agree with each other. We then use both of them to verify (select or reject) the computed CC time delay, that is, to

*Present address: U.S. Geological Survey, 4200 University Drive, Anchorage, Alaska 99508.

check whether the differences between the CC and the two BS estimates are both within a specified limit. This BS verification process can provide both quality control over the chosen CC time delays and potentially more differential travel times for close event pairs. We apply this technique to obtain BS-verified CC differential times for 822 New Zealand earthquakes and relocate 521 of the events using the double-difference (DD) algorithm (Waldhauser and Ellsworth, 2000). We find that the BS-verified CC time delays provide improved (smaller root mean square [rms] residual and more clustered) earthquake relocation results compared to those selected with the threshold criterion.

Bispectrum Method

Let us assume that there are two similar time series $x(t)$ and $y(t)$,

$$x(t) = S(t) + N_1(t)$$
$$y(t) = S(t - D) + N_2(t),$$

where $S(t)$ is an unknown signal and $S(t - D)$ is the same signal delayed (or advanced) in time. $N_1(t)$ and $N_2(t)$ are unknown noise sources (Nikias and Pan, 1988). The basic approach to obtain the time delay D is to shift $x(t)$ with τ lags relative to $y(t)$ and compare the similarity between them with the CC function $R_{xy}(\tau)$. Ideally $R_{xy}(\tau)$ peaks at $\tau = D$ and provides the relative time delay. This, however, is not necessarily true in real applications due to finite-length data records and correlated noise sources.

The CC approach and its variants work in the second-order spectral domain. When the signal $S(t)$ can be regarded as a non-Gaussian stationary process and the noise sources $N_1(t)$ and $N_2(t)$ as two zero-mean correlated Gaussian processes, the similarities between $x(t)$ and $y(t)$ can be better compared in the third-order spectral or BS domain. This BS method takes advantage of the fact that for Gaussian processes all spectra of order higher than two are identically zero. Given $X(\omega)$ and $Y(\omega)$ as the Fourier transforms of $x(t)$ and $y(t)$, the auto-BS $B_{xxx}(\omega_1, \omega_2)$ and cross-BS $B_{xyx}(\omega_1, \omega_2)$ of the two time series can be related to the auto-BS of the signal $B_{sss}(\omega_1, \omega_2)$ as

$$B_{xxx}(\omega_1, \omega_2) \equiv E[X(\omega_1)X(\omega_2)X^*(\omega_1 + \omega_2)] = B_{sss}(\omega_1, \omega_2)$$
$$B_{xyx}(\omega_1, \omega_2) \equiv E[Y(\omega_1)X(\omega_2)X^*(\omega_1 + \omega_2)] = B_{sss}(\omega_1, \omega_2)e^{j\omega_1 D},$$

where $E[\cdot]$ is the expectation operator and X^* is the conjugate of X (Nikias and Raghuveer, 1987; Nikias and Pan, 1988). The effect of correlated noise $N_1(t)$ and $N_2(t)$ is effectively eliminated when we compare the two time series in the BS domain.

Several practical procedures for computing the auto- and cross-BS for two finite-length time series and calculating the time delay between them are given by Nikias and Raghuveer (1987) and Nikias and Pan (1988). The one we adopt for this work can be briefly described as follows:

1. The two time series $x(t)$ and $y(t)$ are both divided into K overlapping data segments. Each segment has M sample points.
2. For the ith data segments $x^i(n)$ and $y^i(n)$ $(0 \le n \le M - 1)$, we calculate the third-order auto and cross cumulants

$$\hat{r}^i_{xxx}(\tau, \rho) = \frac{1}{M}\sum_{k=k_1}^{k_2} x^i(k)x^i(k + \tau)x^i(k + \rho)$$
$$\hat{r}^i_{xyx}(\tau, \rho) = \frac{1}{M}\sum_{k=k_1}^{k_2} x^i(k)y^i(k + \tau)x^i(k + \rho),$$

   where $k_1 = \max(0, -\tau, -\rho)$ and $k_2 = \min(M - 1, M - 1 - \tau, M - 1 - \rho)$.
3. The two cumulants are averaged over the K data segments.
4. A two-dimensional Fourier transform is performed over the two averaged cumulants to obtain the auto-BS $\hat{B}_{xxx}(\omega_1, \omega_2)$ and cross-BS $\hat{B}_{xyx}(\omega_1, \omega_2)$.
5. We then obtain the phase spectra $\hat{\psi}_{xxx}(\omega_1, \omega_2)$ and $\hat{\psi}_{xyx}(\omega_1, \omega_2)$ of the two BSs and calculate the function

$$\hat{I}(\omega_1, \omega_2) = \exp\{i[\hat{\psi}_{xyx}(\omega_1, \omega_2) - \hat{\psi}_{xxx}(\omega_1, \omega_2)]\}.$$

6. The BS-correlation series $\lambda_{xy}(t)$ is obtained by summing $\hat{I}(\omega_1, \omega_2)$ along ω_2 first and then taking the one-dimensional inverse Fourier transform

$$\lambda_{xy}(t) = F^{-1}\left[\sum_{\omega_2}\hat{I}(\omega_1, \omega_2)\right].$$

   The time delay D between the two time series $x(t)$ and $y(t)$ is estimated by locating the lag at which $\lambda_{xy}(t)$ peaks.

Bispectrum Verification

As stated earlier, for different events recorded at the same station, we expect that the noise in their waveforms may be partially correlated or just randomly correlated. Whether the noise is Gaussian or not, however, is arguable because it is hard to separate noise from the true seismic signals and make a statistical analysis. Even if the noise is non-Gaussian, it can still be suppressed by the BS method when it has zero skewness (Nikias and Pan, 1988). Hinich and Wilson (1992) derived the variance of the BS time delay estimate and found that it is asymptotically proportional to the square of the signal skewness and the cube of the signal-to-noise ratio. They further compared it with the variance of the time delay estimated using the cross-power spectrum (similar to CC). They find that for low signal-to-noise ratios and uncorrelated noise, the BS method will not always provide a performance advantage over the cross-power spec-

trum. The BS method, however, has an obvious advantage when correlated noise is present, which results in a bias for the cross-power spectrum (Hinich and Wilson, 1992).

In this work, we do not argue that the BS method always obtains a better time delay estimate than the CC technique in the applications to seismic waveforms recorded at the same station. Rather, our strategy is to test for agreement between the two methods. For an event pair recorded at the same station, we compute two BS time delay estimates using both the raw and bandpass-filtered waveforms. We then use them to verify (select or reject) the one computed with the CC technique using the bandpass-filtered waveforms, that is, to check whether the differences between the CC and the two BS estimates are both within a specified limit (equivalently, we can also use the BS time delay estimates to check the reliability of the one computed with the cross-spectral method). By applying two different methods that work in both the second- and third-order spectral domains, we can improve the reliability of the selected time delay (or related differential times) for earthquake relocation. The two BS time delay estimates do not always agree with each other because the characteristics of noise in the raw and filtered waveforms are different. Therefore checking the values of the CC time delay against both of them provides additional quality control. Another advantage of this practice is that it is very insensitive to the parameters used for bandpass-filtering the waveforms, and therefore it can be advantageous for automated processing.

Figure 1 shows an application example of the bispectrum verification. The waveforms are recorded at station KIW with an epicentral distance of 61 km for a pair of relatively close New Zealand events. The computed CC coefficient is 0.74 (Fig. 1D), which is above the nominal threshold of 0.70 often used for selecting time delays. The CC-determined lag, however, is very different from those obtained with the BS methods (Fig. 1C,D). In this case, the CC-determined time delay is rejected. From the seismic waveforms (Fig. 1A,B), we can see that this is apparently a case of cycle skipping: the filtered waveforms coincidentally correlate slightly better with a lag of -10.

We further observe that for two closely located events, the CC coefficients for their waveforms at several stations may fall below the typical threshold value researchers often set (e.g., 0.70) due to noise contamination. Figure 2 shows an example of the application of the two methods to the waveforms recorded at station OTW with an epicentral distance of 38 km for a different pair of close events. Both methods provide the same correct time delays, but the associated CC coefficient is only 0.50. Under the threshold criterion, such time delay estimates associated with low CC coefficients are simply discarded. Using the BS method, however, we can verify and pick out the reliable time delays from these seemingly not very similar waveforms of two close events, such as those shown in Figure 2, and provide more time control over the relative locations between them.

Algorithm

For the kth common station that provides waveforms for two earthquakes i and j, we rely on the catalog phase picks (P or S) to form the data windows used for time delay calculations. Using the bandpass-filtered waveforms, we first calculate the CC time delay in lag number $\Delta_{ij}^{k(\mathrm{cc})}$. If its associated CC coefficient is large enough, we also perform a subsample time delay calculation to get $\Delta_{ij}^{k(\mathrm{sub})}$ by a coherency-weighted linear fitting of the cross-spectrum phase, after we realign the two windowed waveforms to the closest sample point using $\Delta_{ij}^{k(\mathrm{cc})}$ (Poupinet *et al.*, 1984). Once we complete the CC calculations for all the common stations, we can obtain a maximum CC coefficient $\mathrm{CC}_{ij}^{\max}$ that reflects the extent of waveform similarity for the event pair. Because the BS time delay calculation is computationally demanding—our work indicates that it usually takes more than 10 times the calculation time of the CC technique for the same data—we will only perform the BS estimations for the event pair if its $\mathrm{CC}_{ij}^{\max}$ reaches above a specified threshold. We then compute two additional estimates of time delay in lag number for each common station, that is, $\Delta_{ij}^{k(\mathrm{bs1})}$ using the bandpass-filtered waveforms and $\Delta_{ij}^{k(\mathrm{bs2})}$ with the raw waveforms.

A computed CC time delay $\Delta_{ij}^{k(\mathrm{cc})}$ passes the BS verification if its differences from the two BS estimates $\Delta_{ij}^{k(\mathrm{bs1})}$ and $\Delta_{ij}^{k(\mathrm{bs2})}$ do not exceed a tolerance limit Δ^{lim}. The exact verification process for an event pair varies according to the size of its maximum CC coefficient $\mathrm{CC}_{ij}^{\max}$. We use three threshold CC coefficients to control the process, a central limit $\mathrm{CC}^{\mathrm{lim}}$ that is similar to the threshold value researchers often use to select time delay estimates, a lower limit $\mathrm{CC}^{\mathrm{lim}(l)}$, and an upper one $\mathrm{CC}^{\mathrm{lim}(u)}$. Generally $\mathrm{CC}^{\mathrm{lim}(l)} \le \mathrm{CC}^{\mathrm{lim}} \le \mathrm{CC}^{\mathrm{lim}(u)}$.

1. If $\mathrm{CC}_{ij}^{\max} \ge \mathrm{CC}^{\mathrm{lim}(u)}$, we will verify (select or reject) the CC time delay estimates for those stations with CC coefficients above the lower limit $\mathrm{CC}^{\mathrm{lim}(l)}$. In other words, for an event pair with high extent of waveform similarity, we will choose all the CC time delay estimates with CC coefficients above $\mathrm{CC}^{\mathrm{lim}(l)}$ that pass the BS verification, even though some of them have CC coefficients smaller than $\mathrm{CC}^{\mathrm{lim}}$ and would not be used under the threshold criterion often adopted by other researchers.
2. If $\mathrm{CC}^{\mathrm{lim}} \le \mathrm{CC}_{ij}^{\max} < \mathrm{CC}^{\mathrm{lim}(u)}$, we will make the verifications only for those stations with CC coefficients above $\mathrm{CC}^{\mathrm{lim}}$.
3. If $\mathrm{CC}_{ij}^{\max}$ falls below $\mathrm{CC}^{\mathrm{lim}}$, the CC time delays for the event pair are simply discarded.

Application

Data

We apply the aforementioned BS verification technique to 822 New Zealand earthquakes that occurred in 1996 in the Wellington area (40.8°–41.8° S, 174°–175.7° E). These

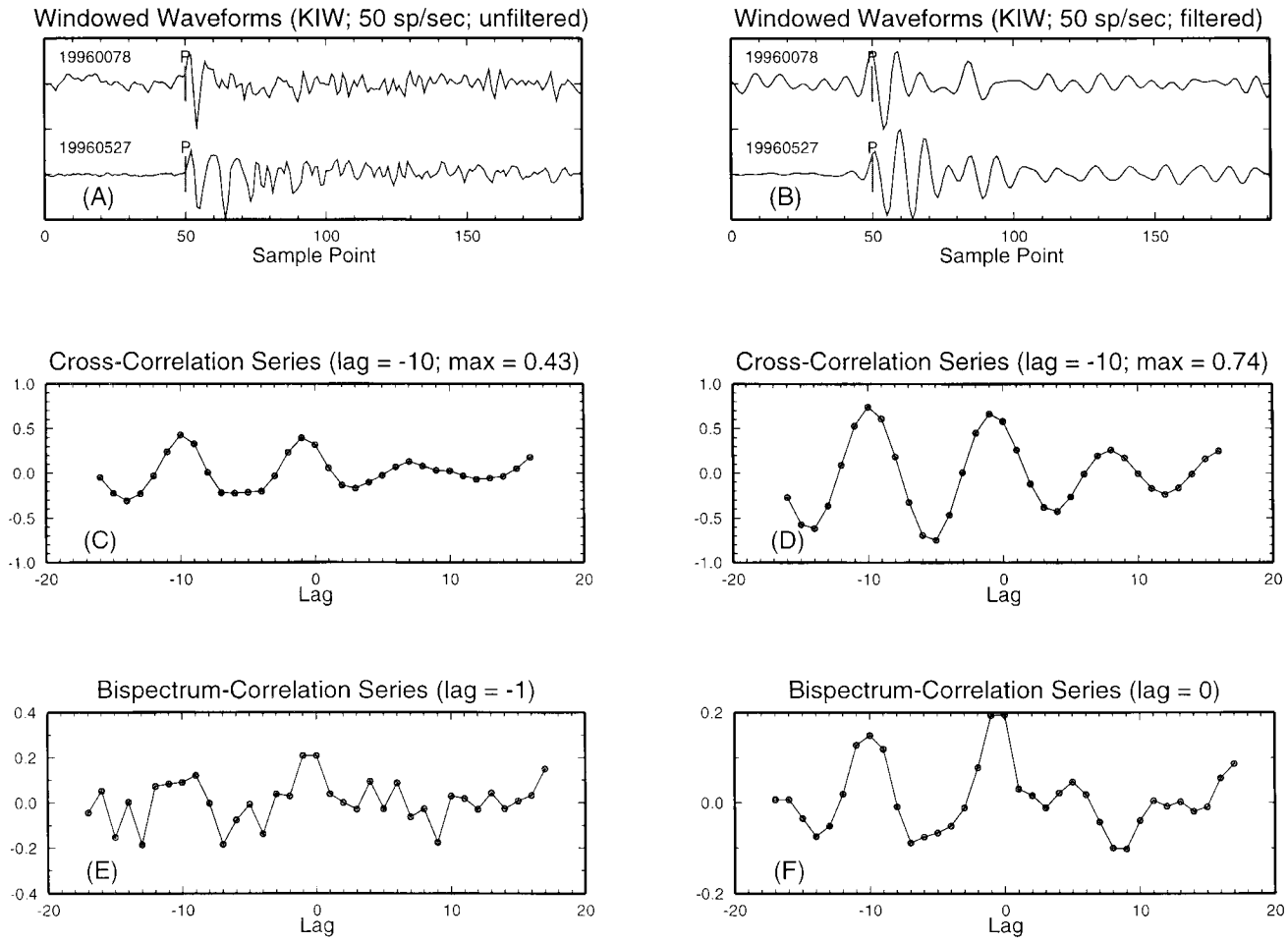

Figure 1. (A) Windowed waveforms (1 sec before and 2.82 sec after the catalog *P* pick) for two New Zealand earthquakes recorded at station KIW with an epicentral distance of 61 km. The station sampling rate is 50 sampling points/sec, and the waveforms are aligned by the *P* picks. (B) Windowed waveforms bandpass filtered between 1 and 6 Hz. (C) CC series for the raw waveforms. (D) CC series for the filtered waveforms. (E) Bispectrum-correlation (BC) series for the raw waveforms. (F) BC series for the filtered waveforms.

events have magnitudes from 2.0 to 4.6, and 35 short-period seismic stations provide waveform data for them. We bandpass filter the waveforms between 1 and 6 Hz. We find that choosing a different filtering range (e.g., 1.5–8 Hz) does not change the final results significantly. A 3.82-sec (1 sec before and 2.82 sec after the catalog phase pick) or 192 sample-point data window is used for the time delay computations.

We adopt the following parameters to choose BS-verified CC time delays: $CC^{lim(l)} = 0.30$, $CC^{lim} = 0.70$, $CC^{lim(u)} = 0.80$, and $\Delta^{lim} = 1$. We compare the results with those obtained using a threshold value of 0.70. Figure 3 shows the distribution of CC time delay estimates with respect to the CC coefficients for both the threshold (Fig. 3A,C) and BS (Fig. 3B,D) selection criteria. A total of 9699 *P*-wave estimates have associated CC coefficients above $CC^{lim} = 0.70$. After the BS verification, that number drops 16% to 8149. An additional 4308 estimates with associated CC coefficients between $CC^{lim(l)} = 0.30$ and 0.70 for event pairs with maximum CC coefficient above $CC^{lim(u)} = 0.80$ pass the BS checking. Together we have 12,457 *P*-wave time delay estimates, which is 28% higher than the number we can obtain using the threshold criterion.

The number of time delay estimates for *S* waves is much smaller than that for *P* waves. One reason is that fewer *S* picks are available in the phase catalog because they are more difficult to pick. The other is that *P*-wave coda tends to contaminate the *S* window we use to measure the time delays and thus decreases the CC coefficient. A total of 3181 *S*-wave time delay estimates have associated CC values above $CC^{lim} = 0.70$, and 76% of them pass the BS checking. Together with those time delays with CC values between $CC^{lim(l)}$ and 0.70, there are a total of 2747 BS-verified time delay estimates for *S* waves. We also examine how the verification percentages for time delay estimates change with

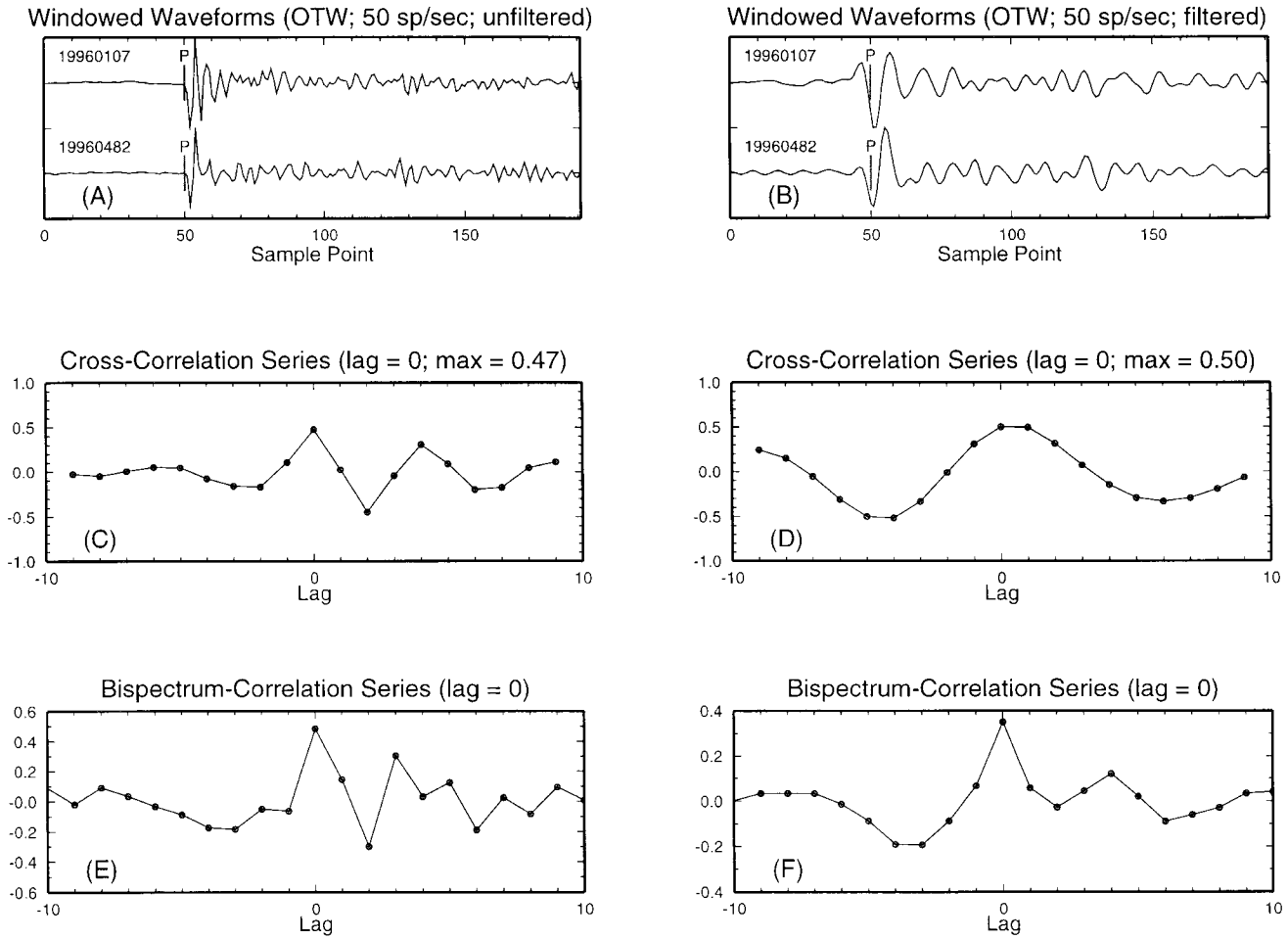

Figure 2. (A) Windowed waveforms (1 sec before and 2.82 sec after the catalog *P* pick) for a different event pair recorded at station OTW with an epicentral distance of 38 km. The station sampling rate is 50 sampling points/sec, and the waveforms are aligned by the *P* picks. (B) Windowed waveforms bandpass filtered between 1 and 6 Hz. (C) CC series for the raw waveforms. (D) CC series for the filtered waveforms. (E) BC series for the raw waveforms. (F) BC series for the filtered waveforms.

the CC coefficients. For both *P* and *S* waves the verification percentage decreases when the CC coefficient becomes smaller, as would be expected. The selection percentages for *P* waves generally are higher than those for *S* waves.

Differential Time Calculation

Using the catalog phase picks at the *k*th station for event pair *i–j*, we can calculate the catalog differential time as

$$\delta t_{ij}^{k(\mathrm{ct})} = (t_i^{k(\mathrm{phase})} - t_i^{\mathrm{o}}) - (t_j^{k(\mathrm{phase})} - t_j^{\mathrm{o}}),$$

where t_i^{o}, t_j^{o}, $t_i^{k(\mathrm{phase})}$, and $t_j^{k(\mathrm{phase})}$ are the origin times and phase (either *P* or *S*) arrival times at the *k*th station for event *i* and *j*, respectively. For the 822 New Zealand earthquakes a total of 39,142 *P*-wave and 11,214 *S*-wave catalog differential times are formed.

When waveform data is available at the *k*th station for event pair *i–j*, we align the two seismic traces by the phase picks and compute the CC time delay $\Delta_{ij}^{k(\mathrm{cc})}$. Then we proceed to calculate the CC differential time as

$$\delta t_{ij}^{k(\mathrm{cc})} = \delta t_{ij}^{k(\mathrm{ct})} + (\Delta_{ij}^{k(\mathrm{cc})} + [\Delta_{ij}^{k(\mathrm{sub})}]) \cdot dt^k,$$

where dt^{k} is the recording time step at the *k*th station.

We further compare the CC and catalog differential times. Their absolute difference in sample points, $|\Delta_{ij}^{k(\mathrm{cc})}|$, as a function of CC coefficients are presented in Figure 4. Both the maximum and mean differences for bins of CC coefficients with width of 0.02 are shown. The mean differences generally decrease with increasing CC values as expected. They are smaller than 6 and 16 sample points (or 0.12 and 0.32 sec) for *P* and *S* waves, respectively. The maximum differences for bins of CC coefficients, however, are much larger than the means for both *P* and *S* waves and show wide fluctuations. Their sizes are larger for *S* waves than for *P* waves because *S* arrivals are picked less accurately than *P* arrivals in general.

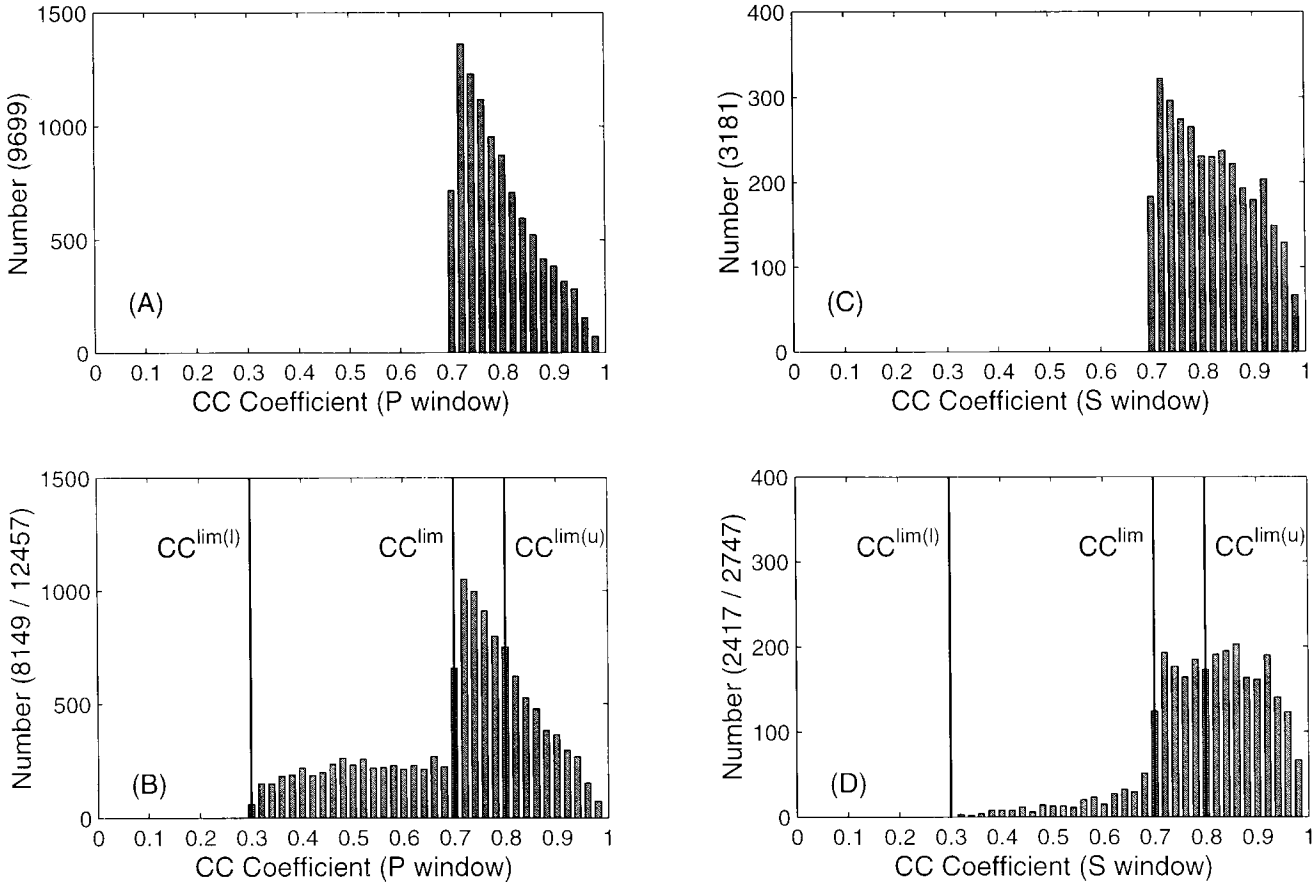

Figure 3. Histograms of selected CC time delay estimates with respect to the CC coefficients for both the threshold (A and C) and BS (B and D) selection criteria for the New Zealand data set. The bin width for CC coefficients is 0.02. The results for *P* waves are shown in A and B, and those for *S* waves are depicted in C and D. The parameters used for BS verification are $CC^{lim(l)} = 0.30$, $CC^{lim} = 0.70$, $CC^{lim(u)} = 0.80$, and $\Delta^{lim} = 1$. The three vertical lines on B and D indicate the positions of $CC^{lim(l)}$, CC^{lim}, and $CC^{lim(u)}$. A total of 9699 *P*-wave (A) and 3181 *S*-wave (C) time delay estimates have associated CC coefficients above $CC^{lim} = 0.70$. After the BS verification they drop to 8149 and 2417, respectively. A total of 12,457 *P*-wave (B) and 2747 *S*-wave (D) CC time delay estimates are selected through the BS verification.

Earthquake Relocation

We adopt the DD algorithm hypoDD (Waldhauser and Ellsworth, 2000) to perform relocation for the 822 New Zealand earthquakes. We use the one-dimensional velocity model Robinson (1986) developed for the Wellington region. Due to hypoDD's criteria for including events, we are able to relocate 521 of the earthquakes (63%). Figure 5 shows in map view the geographic positions of these events before (Fig. 5A) and after (Fig. 5B) relocation. We can see that the relocated seismicity map shows much tighter event clustering. Several event groups after relocation form lineaments that may be associated with the local geological structures. In this work, however, we do not want to explore in more detail the features of the relocated seismicity, because of the limited time frame of the available data. Instead we want to focus on the differences in relocation results obtained from using various sets of data. We carry out the DD relocation with three types of differential time data, that is, catalog data, CC measurements selected with the threshold criterion, and CC measurements verified with the BS method. Because we use the same control parameters for hypoDD, the differences in the relocation results are totally caused by the differences in the input differential time datasets.

The consistencies or qualities of the selected CC differential times for relocation can be examined by their rms residuals. We compile seven threshold-selected differential time data sets using cutoff values from 0.50 to 0.80 with a step increase of 0.05 and 11 BS-verified datasets with the lower limit $CC^{lim(l)}$ increasing from 0.30 to 0.80 with a step of 0.05. (Other parameters are $CC^{lim(u)} = 0.80$ and $\Delta^{lim} = 1$. If $CC^{lim(l)} \leq 0.70$, $CC^{lim} = 0.70$. Otherwise, $CC^{lim} = CC^{lim(l)}$.) No reweighting of the data is performed during relocation to allow direct comparisons (Waldhauser and

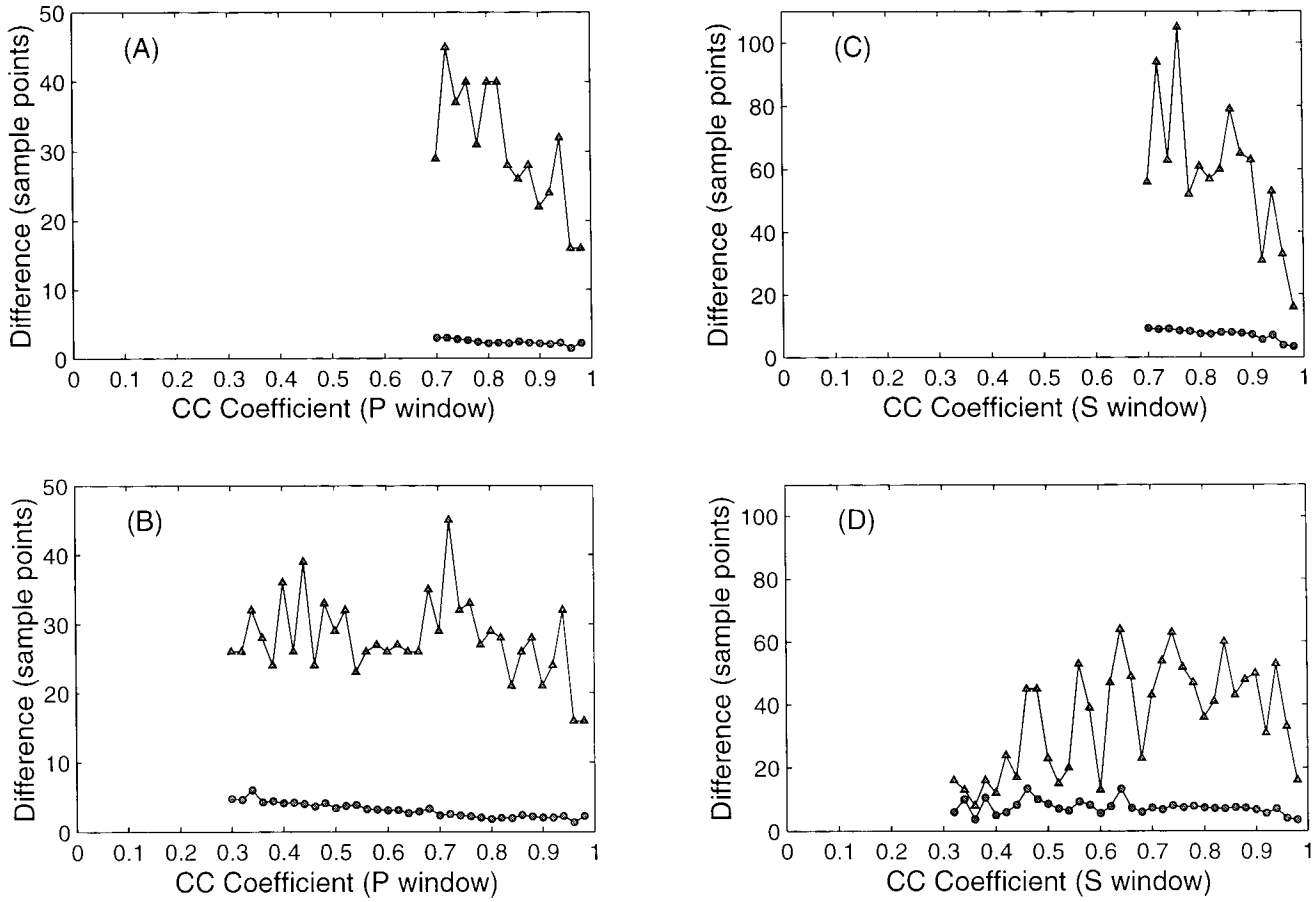

Figure 4. The absolute difference in sample points between the CC and catalog differential times as a function of CC coefficients for the New Zealand data set. The upper (A and C) and lower (B and D) subplots show the results for CC time delays chosen by the threshold and BS selection criteria, respectively. The left (A and B) and right (C and D) subfigures plot the results for *P* and *S* waves, respectively. The mean and maximum lag differences for bins of CC coefficients with width of 0.02 are indicated by circles and triangles.

Ellsworth, 2000). Figure 6 shows the rms residuals for the 19 different sets of differential times (including the catalog data). After five iterations, the rms residual for the catalog data is 145 msec. The rms residuals for the CC differential data selected with the threshold criterion decrease from 149 to 55 msec when the cutoff value increases from 0.50 to 0.80. This pattern is consistent with the expectation that fewer unreliable CC differential time estimates will be included when we raise the threshold value and thus increase the data quality. It further illustrates the importance and difficulty of choosing an optimum cutoff value for the threshold selection criterion (note that by choosing a higher cutoff value, we can improve the quality of the chosen time measurements, but their total number becomes smaller).

The rms residuals for the 11 BS-verified data sets are consistently smaller than their threshold-selected counterparts. This demonstrates that the BS verification process is able to reject those unreliable CC time measurements. The 11 rms residuals have very similar values around 55 msec, suggesting that bispectrum verification performs well on selecting reliable time delay measurements with low CC coefficients. It also means that we do not need to worry much about negatively affecting the quality of the chosen CC time measurements when we decrease the lower limit $CC^{\mathrm{lim}(l)}$ to include additional time constraints for relocation purposes.

We pick out a subregion (enclosed by rectangular boxes in Fig. 5) to illustrate in detail the relocation results obtained with the different data sets. We only show the results for two specific sets of CC differential times depicted in Figure 3, that is, one threshold-selected with a cutoff value of 0.70 and the other BS verified with $CC^{\mathrm{lim}(l)} = 0.30$. Figure 6 shows that the latter has a smaller rms residual after five iterations (61 versus 68 msec). There are 34 earthquakes in the subregion, and they show a very tight depth range (26–28 km) after relocation. Figure 7 shows in sequence (A to D) the geographical positions of the events before and after relocation with three different datasets. Clearly the BS-verified CC differential times (Fig. 7D) provide more clus-

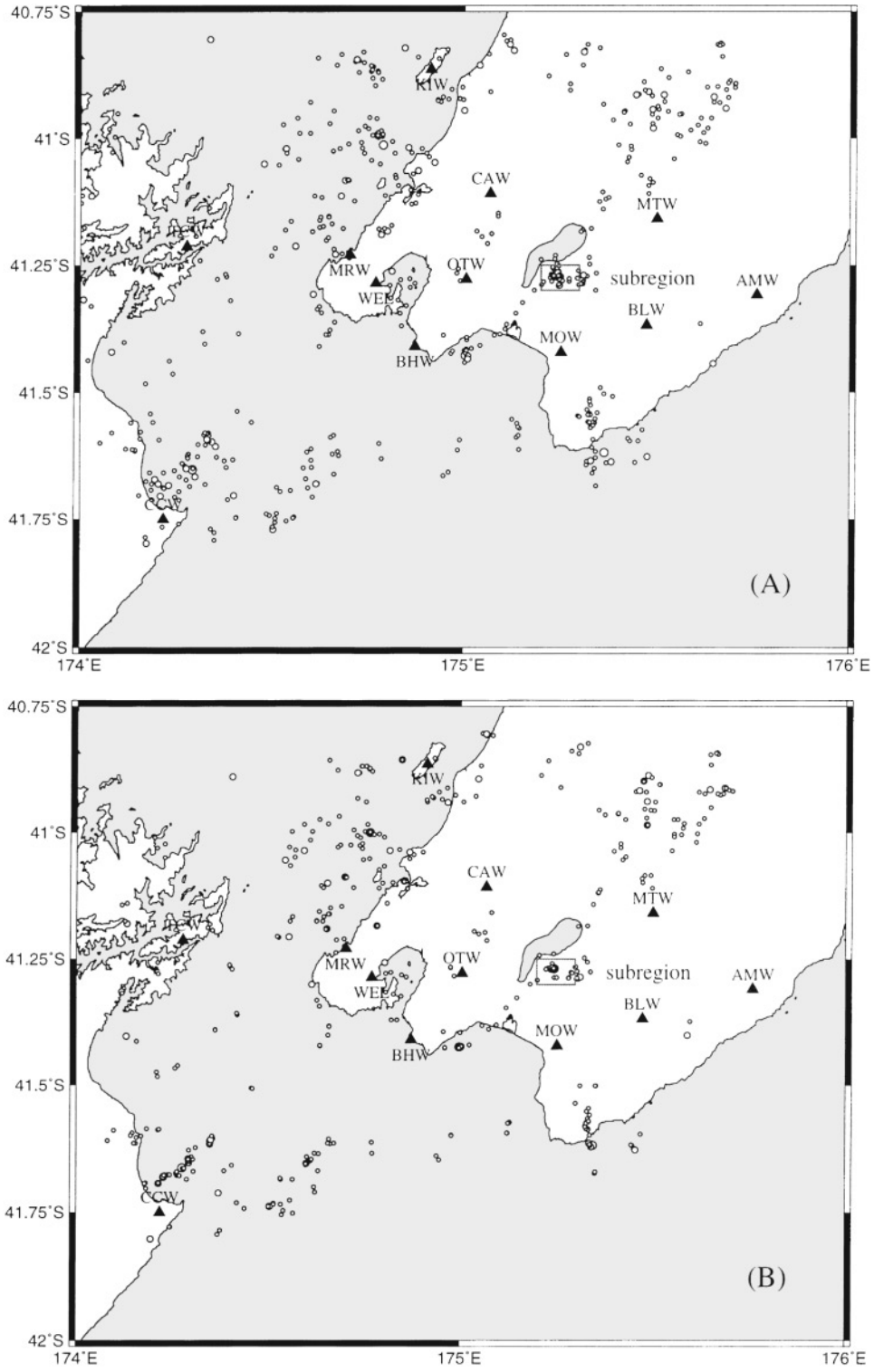

Figure 5. (A) Locations of 521 New Zealand earthquake before relocation. (B) Locations of the same 521 events after relocation using both catalog and CC differential travel times verified with the BS method. Unfilled circles denote the earthquakes, and filled triangles indicate the positions of seismic stations. The rectangular boxes enclose the subregion shown in more detail in Figure 7.

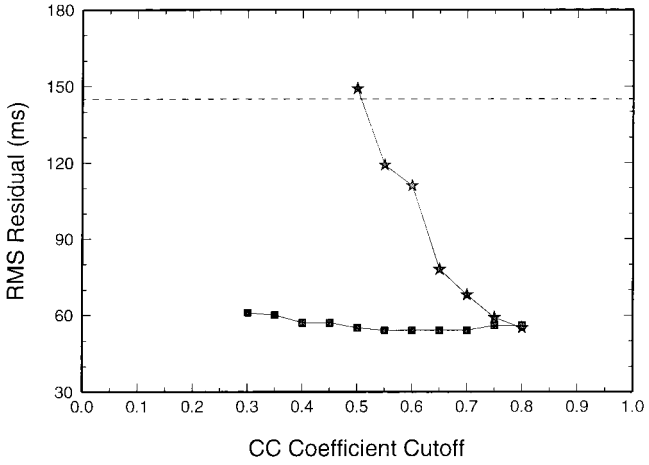

Figure 6. Change of rms residuals with CC coefficient cutoff for the New Zealand data set. The residuals are obtained after five iterations. Values for seven sets of threshold-selected CC differential times are denoted with filled stars and those for 11 sets of BS-verified CC data are represented by filled squares. The horizontal dashed line shows the level of rms residual for the catalog data.

tered results than both catalog data and the threshold-selected one. Figure 8 shows the waveforms (vertical component) of the 34 earthquakes recorded at stations OTW and CAW. The closeness of these events is supported by the high similarities of their waveforms. The improvement from Figure 7C to 7D is expected for two main reasons. First, we are able to get rid of those unreliable CC time delay measurements using the BS checking. Second, the BS verification process can provide more time delay measurements for two close earthquakes and thus more control over their relative positions. This results from the fact that for closely spaced events with high waveform similarities at several stations, the BS verification approach accepts additional time delays at stations with lower waveform similarities or smaller CC values, as long as they pass the checking.

Conclusions

When two similar time series are corrupted by correlated noise sources, the relative time delay between them calculated with the CC technique is sometimes not reliable. The BS method provides an independent check on the CC

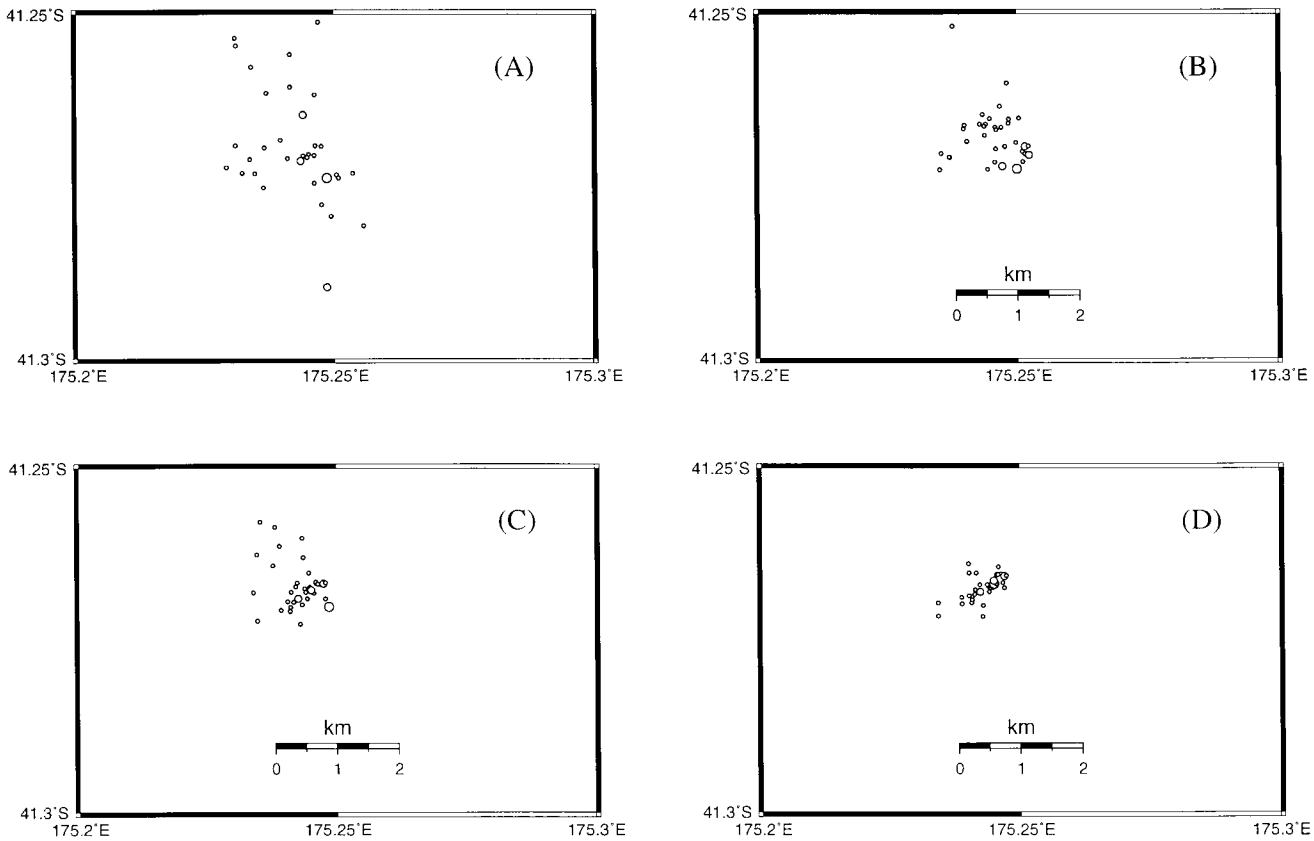

Figure 7. Locations of 34 earthquakes in a subregion (Fig. 5). (A) Before relocation; (B) relocated with catalog differential times; (C) relocated with threshold-selected CC differential times; (D) relocated with BS-verified CC differential times.

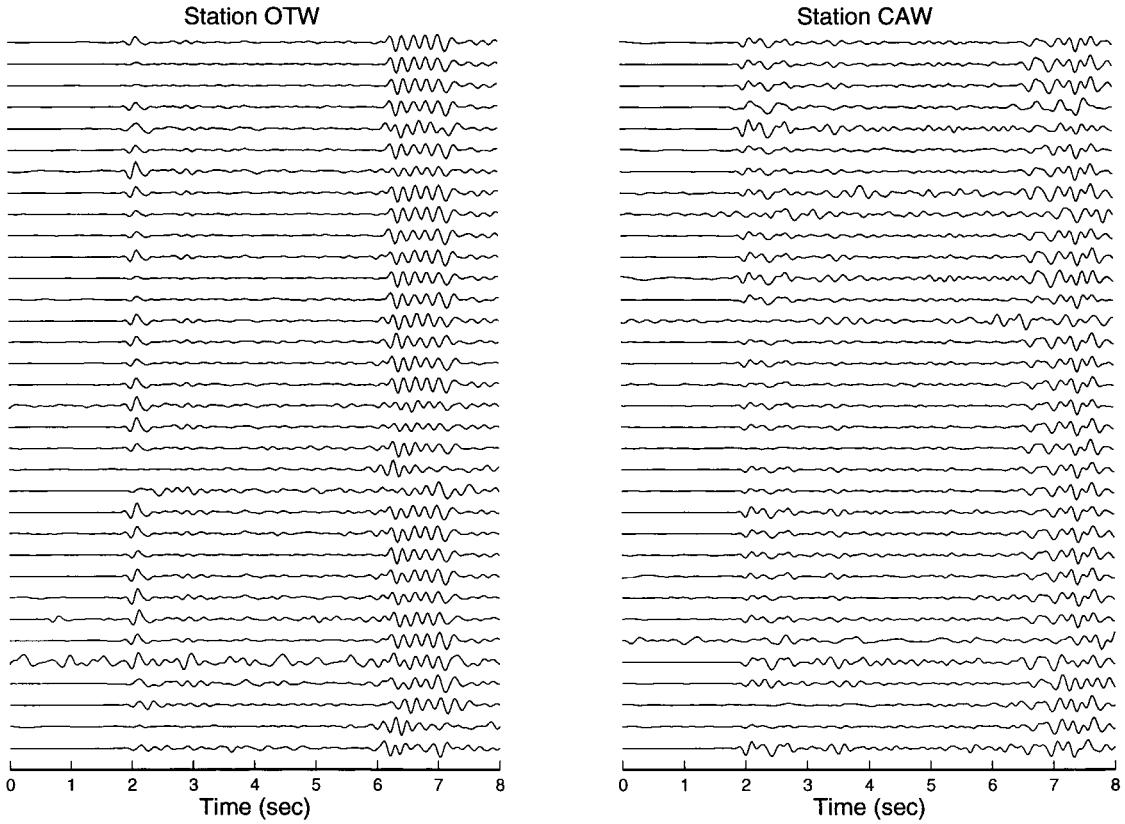

Figure 8. Waveforms (vertical component, bandpass filtered between 1 and 6 Hz) of the 34 earthquakes in Figure 7 recorded at stations OTW and CAW. The time window is 2 sec before and 6 sec after the *P* arrivals.

result by working in the third-order spectral domain. In this work we calculate two more time delays with the BS method, one using the bandpass-filtered waveforms and the other with the raw data, and use them to select the reliable CC estimate computed with the filtered waveforms. We apply this technique to select BS-verified CC time delays or associated differential times for 822 New Zealand earthquakes. We obtain a total of 12,460 BS-verified *P*-wave CC time delays, which is 28% higher than the number we can select using the threshold criterion often adopted by other researchers. We also are able to determine 2747 BS-verified *S*-wave CC measurements. We further perform a DD relocation study and relocate 512 events. The BS-verified CC differential times yield a smaller rms residual than both the threshold-selected CC time measurements and the catalog data, indicating its better quality. It also provides more clustered relocation results than the other two.

Acknowledgments

We acknowledge the careful reviews by Jose Pujol, Peter Shearer, and an anonymous reviewer that helped improve the quality of this manuscript. We thank Xiaodong Song for referring us to the bispectrum method.

This research has resulted from a project supported in part by the Defense Threat Reduction Agency (Contract Number DTRA01-01-C-0085), U.S. Department of Defense; the content does not necessarily reflect the position or the policy of the U.S. government, and no official endorsement should be inferred. This material is based upon work supported in part by the National Science Foundation under Grant Number EAR-0125164.

References

Gillard, D., A. M. Rubin, and P. Okubo (1996). Highly concentrated seismicity caused by deformation of Kilauea's deep magma system, *Nature* **384,** 343–346.

Got, J.-L., J. Fréchet, and F. W. Klein (1994). Deep fault plane geometry inferred from multiple relative relocation beneath the south flank of Kilauea, *J. Geophys. Res.* **99,** 15,375–15,386.

Hinich, M. J., and G. R. Wilson (1992). Time delay estimation using the cross bispectrum, *IEEE Trans. Signal Processing* **40,** 106–113.

Nikias, C. L., and R. Pan (1988). Time delay estimation in unknown Gaussian spatially correlated noise, *IEEE Trans. Acoust. Speech Signal Processing* **36,** 1706–1714.

Nikias, C. L., and M. R. Raghuveer (1987). Bispectrum estimation: a digital signal processing framework, *Proc. IEEE* **75,** 869–891.

Poupinet, G., W. L. Ellsworth, and J. Fréchet (1984). Monitoring velocity variations in the crust using earthquake doublets: an application to the Calaveras fault, California, *J. Geophys. Res.* **89,** 5719–5731.

Robinson, R. (1986). Seismicity, structure, and tectonics of the Wellington region, New Zealand, *Geophys. J. R. Astr. Soc.* **87,** 379–409.

Rowe, C. A., R. C. Aster, W. S. Phillips, R. H. Jones, B. Borchers, and M. C. Fehler (2002). Using automated, high-precision repicking to improve delineation of microseismic structures at the Soultz geothermal reservoir, *Pure Appl. Geophys.* **159,** 563–596.

Rubin, A. M., D. Gillard, and J.-L. Got (1999). Streaks of microearthquakes along creeping faults, *Nature* **400,** 635–641.

Schaff, D. P., G. H. R. Bokelmann, G. C. Beroza, F. Waldhauser, and W. L. Ellsworth (2002). High-resolution image of Calaveras Fault seismicity, *J. Geophys. Res.* **107,** no. B9, 2186, doi 10.1029/2001JB000633.

Shearer, P. M. (1997). Improving local earthquake locations using the L1 norm and waveform cross correlation: application to the Whittier Narrows, California, aftershock sequence, *J. Geophys. Res.* **102,** 8269–8283.

Waldhauser, F., and W. L. Ellsworth (2000). A double-difference earthquake location algorithm: method and application to the northern Hayward Fault, California, *Bull. Seism. Soc. Am.* **90,** 1353–1368.

Department of Geology and Geophysics
University of Wisconsin–Madison
Madison, Wisconsin 53706
(W.-X.D., C.H.T.)

Institute of Geological and Nuclear Science
Private Bag 1930
Dunedin, New Zealand
(D.E.-P.)

Manuscript received 30 April 2003.